

Records of Holocene climatic fluctuations and anthropogenic lead input in elemental distribution and radiogenic isotopes (Nd and Pb) in sediments of the Gulf of Lions (Southern France)

Jean Nizou, Bernard Dennielou, Sidonie Révillon, Maria-Angela Bassetti, Gwenael Jouet, Serge S. Berné, Philippe Nonnotte, Céline C. Liorzou

▶ **To cite this version:**

Jean Nizou, Bernard Dennielou, Sidonie Révillon, Maria-Angela Bassetti, Gwenael Jouet, et al.. Records of Holocene climatic fluctuations and anthropogenic lead input in elemental distribution and radiogenic isotopes (Nd and Pb) in sediments of the Gulf of Lions (Southern France). The Holocene, 2019, 29 (8), pp.1292-1304. 10.1177/0959683619846973 . hal-02331235

HAL Id: hal-02331235

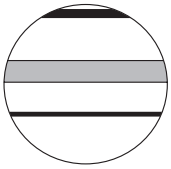
https://univ-perp.hal.science/hal-02331235

Submitted on 24 Oct 2019

HAL is a multi-disciplinary open access archive for the deposit and dissemination of scientific research documents, whether they are published or not. The documents may come from teaching and research institutions in France or abroad, or from public or private research centers.

L'archive ouverte pluridisciplinaire **HAL**, est destinée au dépôt et à la diffusion de documents scientifiques de niveau recherche, publiés ou non, émanant des établissements d'enseignement et de recherche français ou étrangers, des laboratoires publics ou privés.

Check for updates



Research paper

The Holocene
1–13
© The Author(s) 2019
Article reuse guidelines:
sagepub.com/journals-permissions
DOI: 10.1177/0959683619846973
journals.sagepub.com/home/hol
SAGE

Records of Holocene climatic fluctuations and anthropogenic lead input in elemental distribution and radiogenic isotopes (Nd and Pb) in sediments of the Gulf of Lions (Southern France)

Jean Nizou,[1,2] Bernard Dennielou,[1] Sidonie Révillon,[2,3] Maria-Angela Bassetti,[4] Gwenael Jouet,[1] Serge Berné,[4] Philippe Nonnotte[3] and Céline Liorzou[3]

Abstract

Marine mud belts represent potential continuous high-resolution climatic, environmental and anthropogenic archives. In this study, a geochemical record of the Gulf of Lions mud belt, which receives sediments from the Rhône watershed and to a lesser extent from the Languedoc region, is reported from Core KSGC-31. The effects of natural climatic changes and possible anthropogenic disturbances on Holocene sedimentation were ascertained by analysing sedimentation rates, chemical weathering (Al_2O_3/K_2O) and sediment-source shifts (neodymium isotopic ratios; εNd). Measurements of elemental and isotopic lead were used to trace the source and determine the potential vectors of anthropogenic contaminations over the Holocene. High εNd values, recorded from 9000 to 3000 calibrated annum before present (cal. a BP) and around 1500 and 600 cal. a BP, are interpreted as an increase in sediment transport from the Alpine crystalline massifs to the sea induced by enhanced hydro-sedimentary conditions upstream. During the early and middle Holocene, low and stable weathering conditions were persistent, while the late Holocene was characterized by higher and more fluctuating weathering conditions. Sudden changes in the $^{206}Pb/^{207}Pb$ ratio observed during the Roman and Medieval periods suggest clear shifts in lead source from a natural Holocene background to late Holocene anthropogenic contaminations. Even though those shifts are coeval with atmospheric lead contaminations from Spain and Germany recorded in several sediment and ice archives, the local origin (the Cévennes) and the fluvial contamination is more likely in these cases. Those findings are contemporaneous with historical mining records in the Cévennes and point to an intensification of the merchant shipping.

Keywords

Holocene, marine mud belt, medieval lead contamination, Roman lead contamination, sediment source fingerprinting, south of France

Received 19 January 2018; revised manuscript accepted 28 February 2019

Introduction

Disentangling natural and anthropogenic control in Holocene records is subject of intense research efforts. The Holocene climate could be considered as fairly stable in comparison with glacial-interglacial changes; however, several investigations have documented global climatic changes occurring along the Holocene (e.g. Bond et al., 2001; Chapman and Shackleton, 2000; Mayewski et al., 2004; Wanner et al., 2008, 2014). Most of the climatic changes occurred rather simultaneously in several widely distributed records that are characterized by cold conditions at high latitudes and dry conditions at low latitudes (see Mayewski et al., 2004 for a review). Sediment core KSGC-31 is located in the mid-latitude Mediterranean region and therefore bridges the gap between high and low latitudes. The first aspect of this study is to understand how major natural Holocene climate changes influence the sedimentation rates, physical erosion versus chemical weathering and sediment-source shifts in the Gulf of Lions.

Besides the natural influence of climate on the Gulf of Lions sedimentation, Van der Leeuw et al. have observed three major human-induced erosion episodes in the middle and lower Rhône Valley – the first at the end of the Neolithic (~6000 cal. a BP) after the first wave of human expansion, the second at the end of the Bronze Age (~4000 cal. a BP) attributed to a combination of human impact and climate change and the third during the Roman period (~2000 cal. a BP) attributed to changes in the structure of agriculture (Van der Leeuw, 2005). The second aspect of this study is to unravel possible human-induced amplifications of soil degradation using unusual relative increases in physical erosion as well as significant shifts in sediment sources.

[1]IFREMER Unité de Recherche Géosciences Marines, Centre Bretagne – ZI de la Pointe du Diable, France
[2]SEDISOR, IUEM, France
[3]Laboratoire Géosciences Océan LGO UMR 6538, Université de Brest, CNRS, Université Bretagne Loire, Institut Universitaire Européen de la Mer, France
[4]Université de Perpignan, CEFREM, UMR 5110, France

Corresponding author:
Jean Nizou, IFREMER Unité de Recherche Géosciences Marines, Centre Bretagne – ZI de la Pointe du Diable, 29280 Plouzané, France.
Email: jeannizou@gmail.com

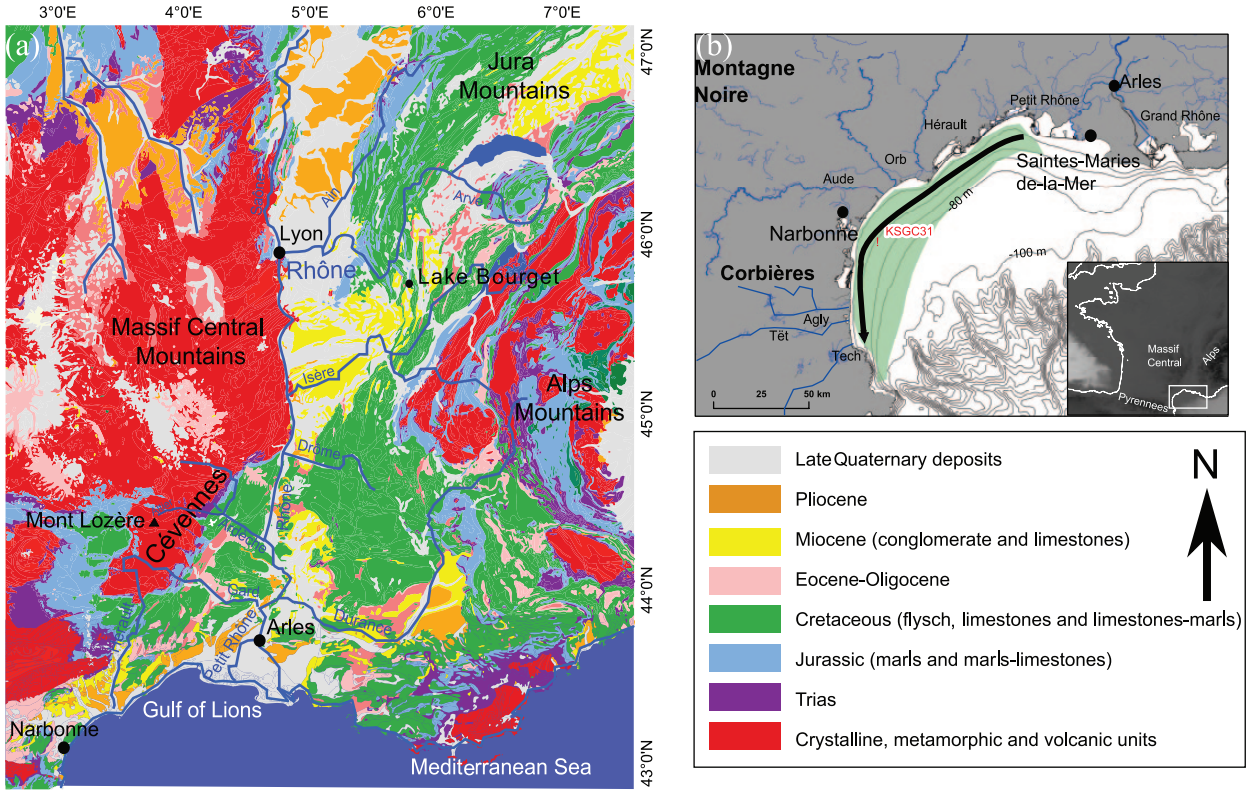


Figure 1. Study area. (a) Simplified geological map redrawn after Révillon et al. (2011). (b) Bathymetric map of the Gulf of Lions, locations of the mud belt (offshore blue facies) and Core KSGC-31 (red star) redrawn after Bassetti et al. (2016). The arrow shows the direction of the cross-shelf sediment transport.

During the Roman period (i.e. 2500–1700 cal. a BP), lead contamination with concentrations four times greater than natural values have been recorded in Swedish lake sediments and Greenlandic ice (Hong et al., 1994; Renberg et al., 1994; Rosman et al., 1997). Lead is a common component of many polymetallic ores. During the flourishing of the Roman civilization, 80 000 metric tonnes of lead were produced per year, approximately the same rate as during the industrial revolution (Settle and Patterson, 1980), by smelting lead–silver alloys in furnaces (McConnell et al., 2018). Since the Roman Empire never reached Swedish and Greenlandic latitudes, the aforementioned authors demonstrated early large-scale atmospheric pollution by lead aerosol particles at a hemispheric scale. Fingerprinting analysis of lead isotopes revealed that the isotopic signature of lead found in Greenlandic ice was consistent with that expected in emissions from southern Spain (Rosman et al., 1997). And yet, ever since, sediment lead pollution originating from Spain and dating to Roman times were recorded in various types of environments such as lagoons (Elbaz-Poulichet et al., 2011), salt marches (Alfonso et al., 2001), harbours (Le Roux et al., 2005), peat bogs (Renberg et al., 2001) all leading to the conclusion that the aerial vector is dominant in these sedimentary environments. With the use of elemental and isotopic lead, the last aspect of this study consists in demonstrating that antique lead contaminations do not uniquely originate from the exploitation of the Spanish mines, and thus suggest an alternative mode of contamination, that is, point-source and fluvial versus diffuse and atmospheric, as well as suggesting, on a larger frame, that lead can be used as a marker of intensification of the merchant shipping.

In order to achieve sufficient time resolution in recording natural and anthropogenic impact on marine sediment composition and contamination over the Holocene, Core KSGC-31 was retrieved from the Gulf of Lions mud belt (Western Mediterranean; Figure 1). Holocene deposits are mainly concentrated in estuaries and prodeltas, but cores from such environments are often discontinuous because of sea-level changes during the Holocene, and/or lateral shifts of depocentres. Mud belts represent interesting sedimentary archives because they generally display a more continuous record of sediment advected by overall circulation from one or several point sources (Hanebuth et al., 2015). Even if accumulation rates are an order of magnitude lower than in estuaries or prodeltas, they generally guarantee more continuous, fine-grained sediment records with minimal hiatuses (see Hanebuth et al., 2015 for a review). The Gulf of Lions mud belt's composition is dominantly supplied by the Rhône River and offers a record of both marine and continental changes documented in three studies that have used Core KSGC-31, namely Bassetti et al. (2016), Jalali et al. (2016) and Sicre et al. (2016). Bassetti et al. (2016) documented decadal to centennial changes in Rhône River hydrological activity by using a multiproxy approach (XRF core scan, grain-size and organic-matter analysis) combined with seismic stratigraphy. While mentioning that more work is needed to unravel anthropogenic from climate control on sedimentation over the late Holocene, the authors came to the conclusion that the elemental composition of marine sediments mainly reflected natural continental erosion and transport. Their work shows a good correspondence with regional paleoclimatological studies and the work of Jalali et al. (2016) regarding temperature variability in the Mediterranean Sea. Jalali et al. (2016) have quantified TERR-alkanes to identify periods of high Rhône River discharge and compare them with regional flood reconstructions. Their results show that concentrations increase from the early Holocene towards the present and that large fluctuations are observed during the late Holocene. In terms of source fingerprinting, the outcome of this study emphasizes that TERR-alkanes mainly reflect inputs from the Northern tributaries of the Rhône River except between 4200 and 2800 cal. a BP. Using the same core, Sicre et al. (2016) have investigated the

multidecadal-scale variability of sea surface temperatures in the convection region of the Gulf of Lions over the past 2000 years using alkenone biomarkers. The present study enhances the comprehension of natural versus anthropogenic control on the sedimentation in the Gulf of Lions through the record of fluctuations of sedimentation rates, chemical weathering (using the Al_2O_3/K_2O ratio; stable vs labile phases) and sediment source shifts (using the neodymium isotopic ratio; εNd). Human lead contaminations were recorded by elemental and isotopic lead to decipher their nature, origin and vector.

Study area

Since the onset of the last deglacial sea level rise ~20 ka ago, sediment depocentres (including the Rhône deltaic and prodeltaic deposits) moved landwards from the shelf break, until sea level stabilization ~7000 cal. a BP ago (Berné et al., 2007; Lambeck et al., 2014; Smith et al., 2011; Figure 1(b)). The change from coastal retrogradation to coastal progradation at the outlet of the Rhône is dated to ~8500–7500 cal. a BP (Arnaud-Fassetta, 1998). Since that time, the Rhône delta experienced several shifts with a net displacement towards the East (Fanget et al., 2014; Jouet, 2007; L'Homer et al., 1981; Vella, 1999). The present-day main mouth channel (Grand Rhône) dates back to AD 1892 (i.e. Anno Domini) and results from the artificial re-opening of a former channel (see Vella et al. (2005) and Fanget et al. (2014) for reviews).

The Gulf of Lions mud belt elongates parallel to the coast between 20 and 90 m water depth, it is 150 km long, 10 to 30 km wide and up to 20 m thick (Figure 1(b)). The morphological characteristics of this sedimentary body are typical of mud belts *sensu stricto* according to the classification of Hanebuth et al. (2015), that is, elongated, parallel to the bathymetry, detached from the point source, covering the inner-, mid-, outer-shelf (Figure 1(b)). Similar mud belts *sensu stricto* are found on the Senegalese shelf (Nizou et al., 2010), on the NW Iberian shelf (Lantzsch et al., 2010) and on the Monterey shelf (Grossman et al., 2006). The composition of the Gulf of Lions mud belt is not well known, but the seismic pattern as well as early mapping has shown that it is dominantly composed of up to 70% bioturbated mud (Aloïsi et al., 1977; Bassetti et al., 2016; Got and Aloïsi, 1990).

At present, the Rhône River provides most of the sediment exported to the Gulf of Lions (estimated ~90% of the total solid fluxes; Dufois et al., 2014; Got and Aloïsi, 1990 and references therein), whereas small rivers of the Languedoc region (Hérault, Orb, Aude, Agly, Têt, Tech; Figure 1(b)) export much less sediment. Three-dimensional numerical modelling of hydrodynamic and sediment transport, together with near-bottom current and suspended sediment concentration measurements show that the mud belt is fed by floods of the Rhône (Ulses et al., 2008). Ulses et al. (2008) have shown that most of the particulate sediment from the Rhône is deposited temporarily in its prodelta, whereas the remaining fraction is transported southwestwards as a river plume whose orientation is controlled by the winds (Mistral, Tramontane and Marin). Another experiment coupled with 3D transport model has shown that during one storm/flood event, about 2.1 Mt of mud (sourced from the Rhône river plume and from re-suspension of prodeltaic mud) can be transported towards the SW and deposited along the mud belt (Dufois et al., 2014). The results of this latter study show that the position of Core KSGC-31 roughly corresponds to the area where sediment deposition along the mud belt during storms is maximum (in the order of 2 cm for one single storm). Finally, it is likely that similar processes occurred since the stabilization of sea level, about 7000 years ago, resulting in the accumulation of the Gulf of Lions mud belt.

In terms of lithologies (Figure 1(a)), the Rhône area can be divided into two end members that are: (1) the mixed sedimentary/crystalline Sub-Alpine and Dauphinois areas and (2) the External Crystalline Alpine Massifs. The Languedoc region displays a mixed sedimentary/crystalline lithology (Révillon et al., 2011). Unlike the Rhône region, where sedimentation (sediment input, erosion/alteration and sediment source shifts) has been intensely studied, little to no information is available on the Languedoc region for the Holocene period.

Material and methods

Core KSGC-31 (IGSN: BFBGX-87912; http://igsn.org/BFBGX-87912) was retrieved from the Rhône mud belt deposit on the Gulf of Lions inner-shelf (43°0′23″N; 3°17′56″E, water depth 60 m; Figure 1(b)). The 7.02 m long core was collected using a piston corer during the GMO2-Carnac cruise in 2002 on the R/V Le Suroît (Sultan and Voisset, 2002).

The age model of the gravity core KSGC-31 is based on 21 radiocarbon dates already published by Jalali et al. (2016) obtained by accelerator mass spectrometry (AMS) performed by the Laboratoire de Mesure du Carbone 14 (Saclay, France) and the Beta Analytic Radiocarbon Dating Laboratory (Florida, US). The ^{14}C dates were converted into 1σ calendar years using Calib7.1 (Stuiver et al., 1998) and the MARINE 13 calibration data set with a reservoir effect of 400 years. The age model and the associated sedimentation rates were obtained by linear interpolation between ^{14}C dates (Jalali et al., 2016). The sediment core spans the last 10 ka BP with little changes in sedimentation rates (Bassetti et al., 2016).

For elemental analyses (Table 1), 20 samples were crushed using an agate mortar. Major and trace elements were determined on the bulk faction at the PSO/IUEM (Pôle Spectrométrie Océan, Institut Universitaire Européen de la Mer, Brest, France), following an analytical procedure modified from Cotten et al. (1995). A quantity of 250 mg of sediment powder were dissolved in closed screw-top teflon vessels (Savillex) at approximately 90°C for one day using 3 ml of concentrated HF, 1 ml of concentrated HNO_3 and 2 ml of concentrated HCl. Then, 94 ml of H_3B0_3 aqueous solution (20 g/L H_3B0_3) were added to neutralize the excess HF. All reagents used are analytical grade. Elements were measured by inductively coupled plasma-atomic emission spectrometry (ICP-AES) using a Horiba Jobin Yvon® Ultima 2 spectrometer. The boron included in the solution was used as an internal standard. Calibrations were made using international standards JSD3, LKSD1, BELC, WSE, CB15, CB18, JB2, ACE. For major elements, relative standard deviation was $\leqslant$1% for SiO_2 and $\leqslant$2% for the other major elements, for trace elements standard deviation was $\leqslant$5%. Loss on ignition value is ~20%. Several indexes of chemical weathering are available, for example, Chemical Index of Alteration (Nesbitt and Young, 1982), Weathering Index of Parker (1970), Weathering Potential Index (Reiche, 1943; modified by Vogel, 1975), Vogt ratio (Roaldset, 1972; Vogt, 1927), Chemical Index of Weathering (Harnois, 1988) that all include in their calculation the CaO of the silicate fraction. Since the bulk (as opposed to decarbonated) sediment samples were used in this study, CaO of the silicate fraction cannot be assessed and therefore Al_2O_3/K_2O was used to estimate stable versus labile phases.

The Avaatech XRF core scanner (Richter et al., 2006) provides semi-quantitative bulk sediment element distribution data. This non-destructive method permits a 1-cm resolution analysis of the chemical composition of Core KSGC-31.

For Nd isotope analyses (Table 1), 20 samples were freeze-dried and wet-sieved at 63 μm to retrieve the fine fraction. Fine fraction was grinded with agate mortar and pestle. Samples were leached with 25 ml of H_2O_2 5% to remove organic matter and with 25 ml of CH_3COOH 10% to remove carbonates. The goal of the leaching is to analyse only the siliciclastic components of the

Table 1. Major element, Nd and Pb isotope compositions in Core KSGC-31.

Core depth (cm)	Age model (cal. a BP)	$^{143}Nd/^{144}Nd$	Error (2σ)	ε Nd (CHUR = 0.512638; Jacobsen and Wasserburg, 1980)	$^{206}Pb/^{204}Pb$	Error (2σ)	$^{207}Pb/^{204}Pb$	Error (2σ)	$^{208}Pb/^{204}Pb$	Error (2σ)	Al_2O_3 (%)	K_2O (%)	Loss on ignition (LOI; %)	Recalculated Al_2O_3 (%)	Recalculated K_2O (%)
9	0	0.512087	8.00E−06	−10.75	18.685	2.770E−04	15.667	2.843E−04	38.750	8.290E−04	11.94	2.20	21	11.80	2.17
55	598	0.512115	4.00E−06	−10.20	18.726	1.997E−04	15.670	2.679E−04	38.778	8.046E−04	11.53	2.26	20	11.43	2.24
70	835	0.512096	6.00E−06	−10.57	18.661	3.507E−04	15.671	3.124E−04	38.720	8.816E−04	12.04	2.10	20	12.13	2.11
88	911	0.512104	6.00E−06	−10.42	18.659	3.692E−04	15.668	3.838E−04	38.729	1.162E−03	11.52	2.14	21	11.55	2.15
99	950	0.512099	6.00E−06	−10.51	18.580	3.727E−04	15.655	3.393E−04	38.602	9.980E−04	11.79	2.31	21	11.74	2.30
118	1078	0.512099	8.00E−06	−10.51	18.802	2.856E−04	15.671	3.004E−04	38.821	8.911E−04	11.34	2.14	21	11.33	2.14
144	1356	0.512112	4.00E−06	−10.26	18.788	3.433E−04	15.673	2.763E−04	38.828	8.664E−04	11.92	2.39	20	11.84	2.37
173	1666	0.512112	6.00E−06	−10.26	18.764	3.310E−04	15.672	2.996E−04	38.807	9.395E−04	11.31	2.16	20	11.18	2.14
198	1968	0.512091	8.00E−06	−10.67	18.668	4.198E−04	15.669	4.413E−04	38.739	1.299E−03	11.44	2.28	21	11.32	2.25
223	2294	0.512098	4.00E−06	−10.53	18.866	4.548E−04	15.671	4.540E−04	38.879	1.267E−03	10.80	2.18	22	10.60	2.14
252	2688	0.512101	8.00E−06	−10.48	18.852	4.045E−04	15.671	3.393E−04	38.862	1.040E−03	11.43	2.12	20	11.50	2.14
273	2986	0.512122	8.00E−06	−10.07	18.882	2.401E−04	15.672	2.878E−04	38.892	9.220E−04	10.72	2.10	21	10.72	2.10
307	3469	0.512113	4.00E−06	−10.24	18.893	2.912E−04	15.672	3.304E−04	38.903	9.822E−04	10.96	1.95	21	11.04	1.96
348	3988	0.512109	6.00E−06	−10.32	18.888	4.629E−04	15.671	4.781E−04	38.890	1.381E−03	10.05	2.00	22	9.94	1.98
361	4127	0.512113	4.00E−06	−10.24	18.867	2.662E−04	15.671	2.292E−04	38.872	7.527E−04	10.19	1.81	22	10.23	1.81
380	4450	0.512111	6.00E−06	−10.28	18.856	3.948E−04	15.674	3.723E−04	38.878	1.158E−03	10.38	2.11	22	10.30	2.10
461	5898	0.512125	6.00E−06	−10.01	18.896	4.116E−04	15.672	4.179E−04	38.909	1.255E−03	10.04	2.02	22	9.91	1.99
507	6922	0.512127	8.00E−06	−9.97	18.864	3.921E−04	15.670	3.712E−04	38.869	1.055E−03	10.57	2.11	22	10.47	2.09
556	7735	0.512112	6.00E−06	−10.26	18.891	4.028E−04	15.670	3.435E−04	38.885	1.023E−03	9.58	1.88	23	9.49	1.86
621	8598	0.512111	4.00E−06	−10.28	18.875	3.209E−04	15.669	3.340E−04	38.867	1.066E−03	9.90	2.00	23	9.60	1.94

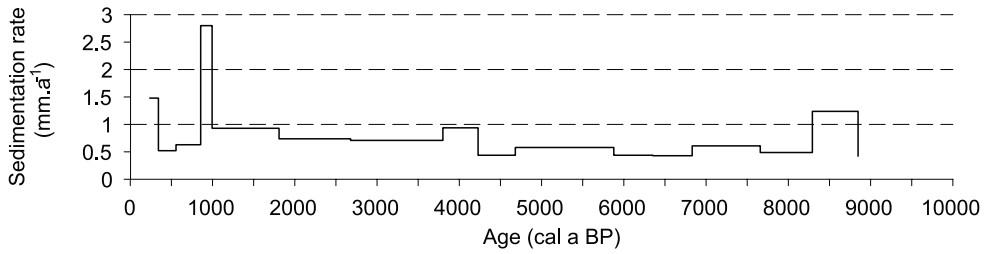


Figure 2. Sedimentation rates against age in Core KSGC-31.

sediment. The samples were prepared following HF + HNO_3 + $HClO_4$ acid digestion (Révillon and Hureau-Mazaudier, 2009). Afterwards, they were evaporated to dryness and dissolved in HCl and HNO_3 overnight. After evaporation, samples were dissolved in HNO_3 1M and were loaded on ion exchange columns for Nd and Pb chemical separation following usual procedures of Pin and Santos Zalduegui (1997) and Deniel and Pin (2001). Nd isotope compositions were measured on a Thermo Scientific TRITON multi-collector TIMS at the PSO. $^{143}Nd/^{144}Nd$ was normalized to $^{146}Nd/^{144}Nd = 0.7219$. International reference standard solution gave average values of $^{143}Nd/^{144}Nd = 0.511849 \pm 0.000003$ (n = 3) for La Jolla (recommended value, 0.511850). Nd isotope results are expressed as: $\varepsilon Nd = (((^{143}Nd/^{144}Nd_{(measured)}/^{143}Nd/^{144}Nd_{(CHUR)}) - 1) \times 10^4$. The Chondritic Uniform Reservoir (CHUR) value is 0.512638 (Jacobsen and Wasserburg, 1980). Analytical errors are reported as 2σ (Table 1). Pb isotope composition measurements were performed at the Pôle Spectrométrie Océan using a Thermo Scientific Neptune multi-collector ICPMS (Table 1). Pb isotope ratios were corrected for instrumental mass fractionation and instrument bias by the Tl doping method of White et al. (2000) and SRM981 Pb standard bracketing every two samples. Pb isotope reproducibility, based on 11 replicate analyses of NIST SRM981 is 16.927 ± 0.0003 (2σ) for $^{206}Pb/^{204}Pb$, 15.478 ± 0.0004 (2σ) for $^{207}Pb/^{204}Pb$ and 36.656 ± 0.0013 (2σ) for $^{208}Pb/^{204}Pb$.

Results

From the early Holocene until 4000 cal. a BP, the recorded sedimentation rates (Figure 2) show a mean value of ~0.5 mm a^{-1}, whereas since 4000 cal. a BP it increased to about ~0.8 mm.a^{-1}. One interval from 992 to 851 cal. a BP shows a sedimentation rate four times greater than the Holocene background. However, since this value is only supported by two dates contained within a small-time window of less than 150 a with respect to the associated 1 sigma error of ± 100 a, this high sedimentation rate value is thus not considered relevant (Figure 2). The Al_2O_3/K_2O ratio (Figure 3(a)) shows two major trends that are as follows: a low and steady state from 9000 to 4200 cal. a BP with values ranging from 4.9 to 5.1 and high-frequency fluctuations with higher average values ranging from 4.9 to 5.8. With respect to the scarcity of the data points and the replication limit (0.35 εNd unit), εNd shows two major trends: a steady state around −10 from 9000 to 3000 cal. a BP, followed by fluctuations within a lower εNd mean range until present (Figure 3(e)). From 3000 cal. a BP to present, two peaks (>0.5 εNd unit) are observed around 1500 and 600 cal. a BP reaching values of −10.2 (Figure 3(e)). The elemental Pb semi-quantitative XRF-scanner- based data (Figure 4(a)) shows a steady state from 9000 to 2500 cal. a BP, followed by a general increase until present with two maxima around 2000 and 800 cal. a BP. As for elemental Pb semi-quantitative data, $^{206}Pb/^{207}Pb$ (Figure 4(b)) shows two trends, a steady state from 9000 to 2500 cal. a BP around 1.204, followed by a general decreasing trend over the past 2500 years. Two minima, 1.192 at 2000 cal. a BP and 1.186 around 1000 cal. a BP are observed.

Discussion

Natural climatically controlled Holocene sedimentation

At the scale of the Holocene, the Gulf of Lions mud belt contains integrated records of the whole Rhône watershed and also to some extent the Languedoc region, which allow identification of a major change in sedimentation centred around 4000/3000 cal. a BP. Even though the resolution of our marine sedimentation rates does not allow us to unravel short-time fluctuations, a small, but significant increase in mean value from ~0.5 to ~0.8 mm.a^{-1} has, however, been recorded around 4000 cal. a BP (Figure 2). Regarding chemical alteration versus physical erosion, the Al_2O_3/K_2O (Figure 3(a)) and K/Ti (Bassetti et al., 2016; Figure 3(b)) ratios show a low and steady state from 9000 to 4200 cal. a BP indicating low weathering conditions. These results are consistent with lacustrine records from the Rhône region, such as the predominance of physical erosion recorded in Lake Bourget interpreted as dry conditions (Arnaud et al., 2012). The Al_2O_3/K_2O record shows overall higher and more fluctuating values from 4200 cal. a BP onwards (Figure 3(a)), indicating higher chemical weathering. This is consistent with higher K/Ti ratio values (Figure 3(b)) interpreted as an intensification of the hydrological activity by Bassetti et al. (2016). Likewise, biomarker data (Jalali et al., 2016; Figure 3(c)) show large fluctuations of TERR-alkane concentrations, also interpreted as enhanced flood activity during the late Holocene. Regarding sediment provenance, an increase in flood frequency in lacustrine sediments from Southern Alpine lakes is also recorded around 4200 cal. a BP (Wirth et al., 2013; Figure 3(d)). The same pattern is observed with subtle changes in Neodymium isotopic compositions along KSGC-31. More radiogenic values are observed during the Mid-Holocene (i.e. εNd ~−10) than during the late Holocene (i.e. εNd ~−10.5) with a major change centred around 3000 cal. a BP (Figure 3(e)). A change starting at 4000 cal. a BP could be observed; however, it cannot be interpreted since the fluctuations observed are contained within the replication limit. The 0.6 εNd unit drop from −10.1 at 3000 cal. a BP to −10.7 at 2000 cal. a BP (Figure 3(e)) suggests a change from a Mid-Holocene stable sediment source supply towards a late Holocene fluctuating source-shift supply.

The sediments deposited at the KSGC-31 core site originate from two regions that are the Rhône and the Languedoc. Both regions are composed of a combination of crystalline and sedimentary rocks that form a cluster of close Neodymium isotopic composition values centred around −10 (Révillon et al., 2011). One must keep in mind that unravelling the Rhône and the Languedoc sources is not possible since they are too close in terms of Neodymium isotopic compositions. Nevertheless, among the Gulf of Lions sediment sources, sediments originating from the Mont-Blanc massif area present striking differences in terms of Neodymium isotopic compositions (i.e. εNd = −5; Révillon et al., 2011). εNd fluctuations in the mud belt are explained in terms of mixing proportions between a less radiogenic background sedimentation and an episodic more radiogenic Alpine source. Since we do not possess quantitative fluxes to discuss

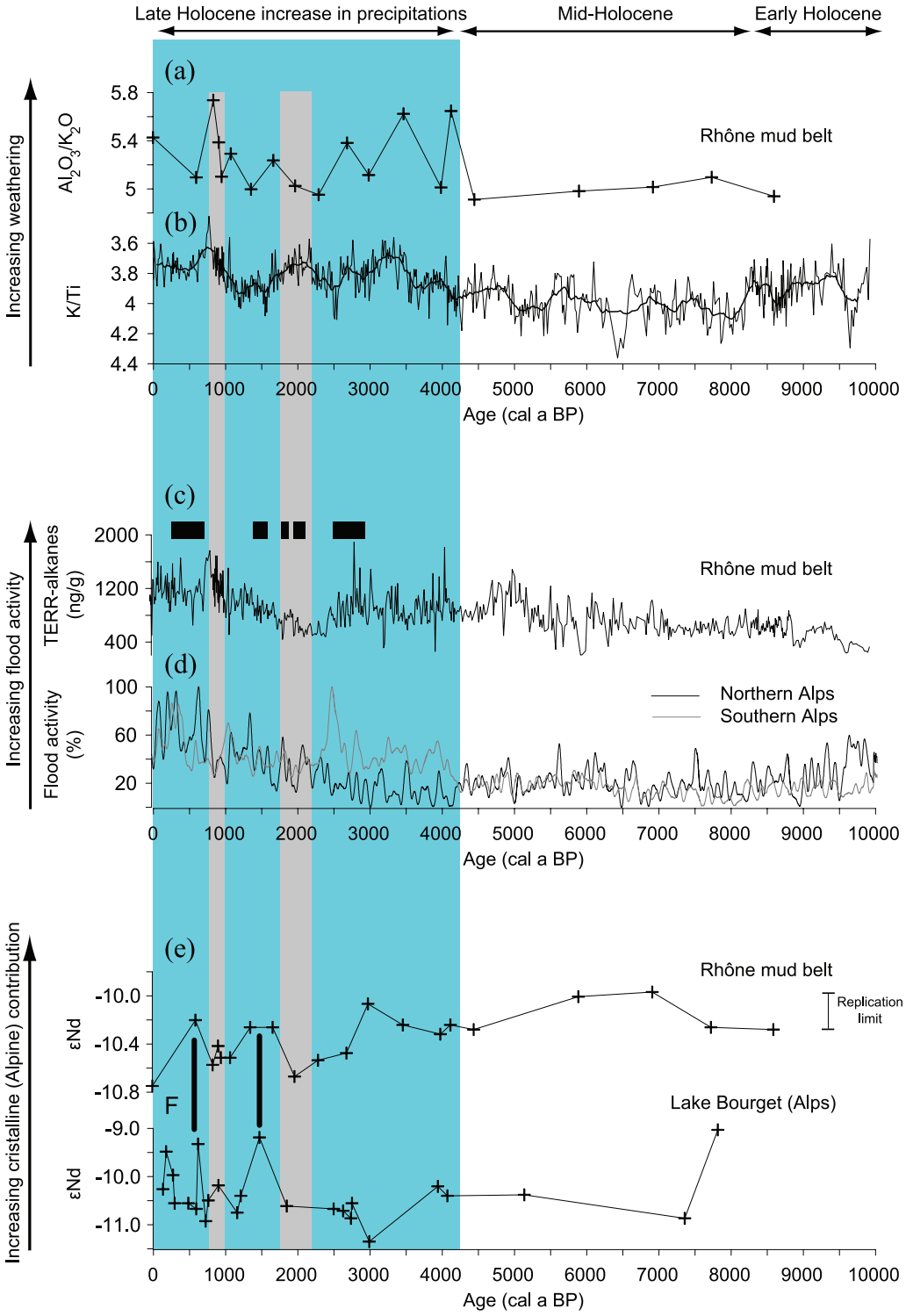


Figure 3. Chemical weathering ascertained by (a) quantitative ICP-AES-derived Al_2O_3/K_2O ratio, and (b) semi-quantitative XRF core scanner-derived K/Ti (Bassetti et al., 2016) in Core KSGC-31 against age. Increase in flood activity ascertained by (c) TERR-Alkanes as a proxy for periods of Rhône avulsion (Jalali et al., 2016) in Core KSGC-31, and (d) North versus South Alpine flood records (Wirth et al., 2013) against age. Periods of high flood activity in the Upper Rhône catchment (Arnaud-Fassetta et al., 2010) are materialized by thick black bars. Sediment source shifts recorded by (e) εNd in Core KSGC-31 is compared to (f) εNd in the Lake Bourget (Arnaud et al., 2012) against age; εNd peak to peak correlations are highlighted by two black bars. Grey bars materialize the periods of Pb sediment contamination recorded in KSGC-31, by both an increase in concentration and a sedimentary source shift (Figure 4).

absolute variations, the observed more radiogenic εNd values during the early and middle Holocene can either be explained by a relative increase in Alpine crystalline massif input or by a relative decrease in sediment input originating from the less radiogenic background. At the scale of the European Alps, there is a consensus that Alpine glaciers in the early and middle Holocene were more retreated than today (see Arnaud et al., 2016 for a review). In that regard, the work of Ivy-Ochs et al. (2009) concerning the European glacier extension have shown that warm conditions prevailed almost continuously until about 3.3 cal, a BP, possibly allowing sedimentary input from the Alpine crystalline massifs to reach KSGC-31 core site (Figure 3(e)).

At a finer time-scale during the late Holocene, taking into consideration the dating uncertainty, the scarcity of the data points

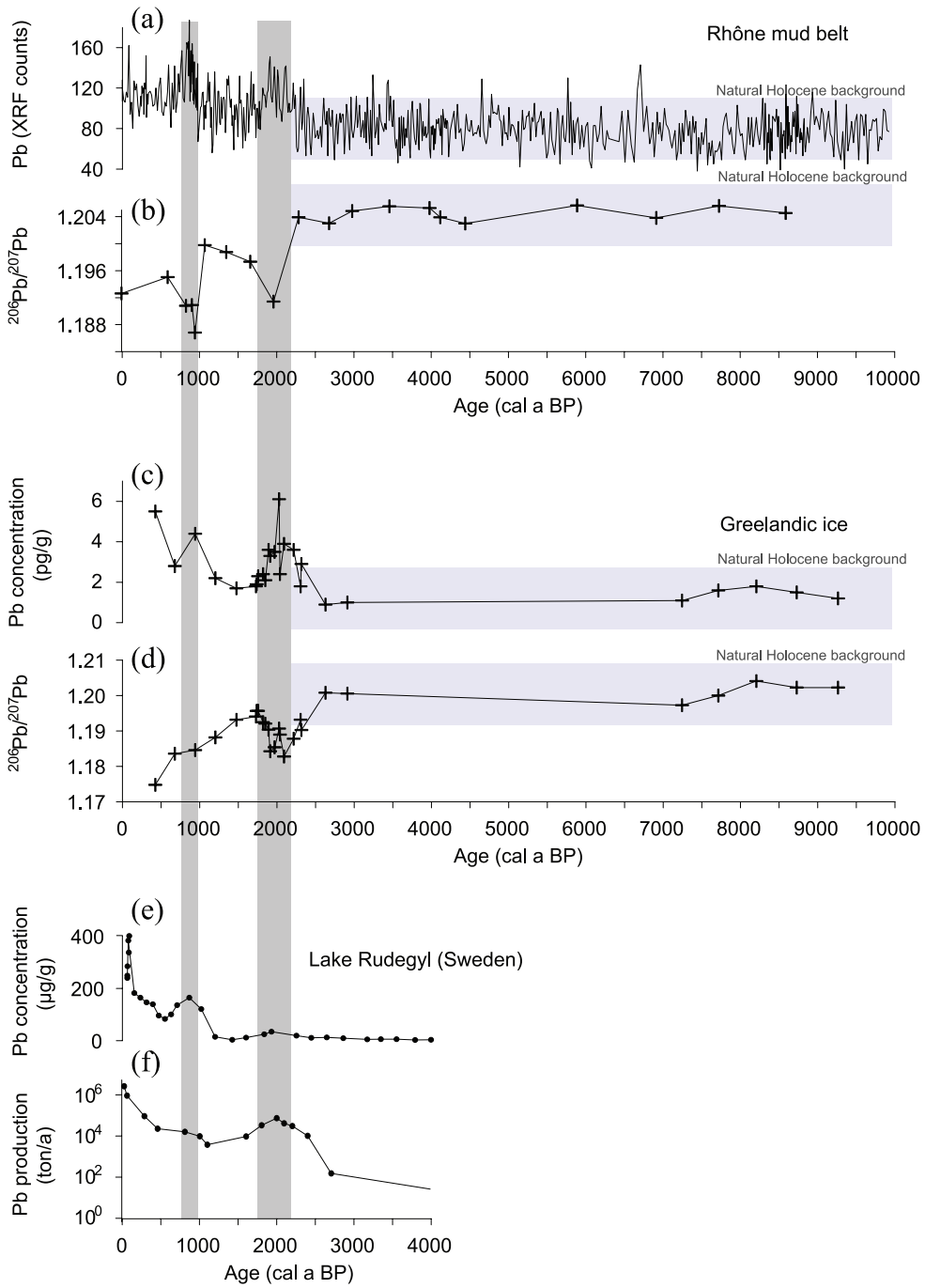


Figure 4. Lead contamination ascertained by (a) semi-quantitative XRF core scanner-derived elemental concentrations, (b) $^{206}Pb/^{207}Pb$ isotopic ratio against age in sediment Core KSGC-31 compared to Greenlandic ice core records of (c) concentrations of lead (Hong et al., 1994) and (d) $^{206}Pb/^{207}Pb$ isotopic ratio (Rosman et al., 1997). Concentrations of lead recorded in Sweden (Lake Rudegyl; redrawn from Renberg et al., 1994; (e) Changes in worldwide lead production over the past 4000 years (redrawn from Settle and Patterson, 1980; (f). Periods of human-induced source shifts are materialized by dark grey bars. Periods displaying the natural Holocene background are underlined by light blue squares.

and the fact that our marine record is integrated over several regions, two increases in εNd are observed around 1500 and 600 cal. a BP (εNd ~−10.2; Figure 3(e)). Those increases, interestingly, match two rises in terrigenous supply recorded in Lake Bourget. In Lake Bourget, two rises in terrigenous flux as well as sedimentary source shifts towards the Mont Blanc crystalline massif are recorded from 1600 to 1300 cal. a BP and from 800 to 50 cal. a BP (Arnaud et al., 2012; Figure 3(f)). The resolution of KSGC-31's record does not allow us to interpret sedimentation rates in a manner that would elucidate quantitative increases in clastic supply for those periods (Figure 2). In the Northern part of the French Alps, Arnaud et al. (2016) highlighted that changes in terrigenous supply in Lake Bourget have been mainly driven by hydrological conditions. The more radiogenic values recorded around 1500 and 600 cal. a BP are concomitant with periods of increases in flood frequency in the Northern Alps (Arnaud-Fassetta et al., 2010; Figure 3). This could explain more radiogenic material being transported from the crystalline Alpine region during enhanced flood activity located upstream; however, dating uncertainty on those short-term events does not allow us to come to a definite conclusion in that regard.

Possible human-induced soil disruptions

Considering the time period, possible human impact on soil disruption may explain high-frequency fluctuations of Al_2O_3/K_2O

and εNd as well as the increase in sedimentation rate observed from 4000/3000 cal. a BP onwards. This highly-debated scientific question has been mentioned in the marine record (using Core KSGC-31) by Bassetti et al. (2016) regarding a possible amplification of soil degradation following waves of human occupation. In continental records in the Southern Alps, Brisset et al. (2013) have shown that even though human activities have had a direct impact on persistent sediment availability at least since 3000 cal. a BP, human pressures could not explain the sharp change in soil cover that they have observed at 4200 cal. a BP. This hypothesis has been suggested in the Northern Alps by Bajard et al. (2016) who have shown that a first erosive phase was initiated around 4500 cal. a BP; however, the first evidences of human presence linked to forest clearance in the catchment were only dated around 3000 cal. a BP. The representativeness of those inherently locally confined records might be questioned. Arnaud et al. (2016) has shown, using a holistic approach that recent Bronze Age agricultural practices did not generate substantial deforestation or erosion in low altitudes. However, at higher altitudes the reinforcement of pastoral activities led to a marked rise in physical erosion intensity that made those environments more sensitive to climate oscillations. By comparing several records across the Alps from the early/middle Bronze Age, Gauthier et al. (2008) and Jacob et al. (2008) have hypothesized that the onset of millet cultivation coincided with the arrival of innovative agricultural practices, such as the improvement of agricultural tools that allowed deeper ploughing in soils. In the Alpine region, copper exploitation activity has been identified by traces of fire during the Bronze Age period from ~ 4350 cal. a BP in the Southern and ~ 4200 cal. a BP in the Western French Alps. Although, mining activities were restricted to small areas, some authors have stated that development of metallurgy above 2000 m altitude may have affected the altitude of the tree-line, pedological processes and/or runoff, in addition to pastoral activities (Simonneau et al., 2014 and references therein).

Lead concentrations and isotope compositions are used as a proxy that is essentially independent from natural sedimentary fluxes. In the late Holocene, even though lead contamination and soil erosion are two fundamentally disconnected processes, our marine record integrated over several regions shows rather sharp and concomitant variations of εNd as well as elemental and isotopic lead around 2000 and 1000 cal. a BP (Figure 3(e)). The less radiogenic εNd values correspond to an increase in contribution of sediments originating from the Rhône and Languedoc regions relative to the crystalline Alpine massifs, and yet in the late Iron Age, several lake records such as Lake Moras (Doyen et al., 2013), Lake Paladru (Simonneau et al., 2013) and Lake Anterne (Giguet-Covex et al., 2011), display an unprecedented rise in erosion that has been attributed to human activities (see Arnaud et al., 2016 for a review). However, it should be noted that in the case of Lake Moras as well as Lake Paladru, both unusual increases in clastic supply are inferred by semi-quantitative XRF-based Ti fluctuations that we do not observe in our quantitative Al_2O_3/K_2O record. Furthermore, the period around 2000 cal. a BP displays a flood-dominated regime recorded in the Rhône deltaic plain by several geomorphological studies (Arnaud-Fassetta, 2002; Arnaud-Fassetta et al., 2010; Bruneton et al., 2001).

Nature and vector of the major anthropogenic lead contaminations

Two $^{206}Pb/^{207}Pb$ drops showing a clear change in lead source (Figures 3 and 4) occurred during the beginning of the Roman Empire and the beginning of the High Middle Ages. However, paradoxically, we do not observe conclusive proof of human-induced soil disruptions evidenced by unusual εNd and Al_2O_3/K_2O values (Figure 3). The $^{206}Pb/^{207}Pb$ drop from 1.204 to 1.192 around 2000 cal. a BP observed in KSGC-31 record (Figure 4(b)) resembles in timing and amplitude the observations made by Rosman et al. (1997; Figure 4(d)) in Greenlandic ice. This has been attributed to large-scale atmospheric pollution originating from the Carthaginian and Roman Spanish Mines. Such contamination by this toxic metal, recorded by both an increase in concentration (Figure 4(a)) and a source shift (Figure 4(b)), without strong evidences of human-induced soil disruptions (clearing/burning woods for smelting and excavation for mining) could be explained by long-distance wind contamination. However, the role of long-range atmospheric transport might be lowered compared to the direct fluvial source, since the Gulf of Lions shelf sedimentation is to a large extent under the influence of the Rhône river discharge (Dufois et al., 2014), and thus the majority of the sediment deposited at KSGC-31 core site runs through the city of Arles. The city of Arles was built in the 6th century BC (~2500 cal. a BP) and achieved prosperity from 49 BC (1999 cal. a BP), when they pledged allegiance to Julius Caesar and remained flourishing until the 2nd century AD (~1750 cal. a BP; Long, 2009). This fits exactly the timing of anthropogenic lead contamination (Figure 4(a) and (b)). And yet in Arles, recovery and recycling of metal was a full-fledged commercial activity (Arles Antiquity Museum). During the Roman Period, raw metal was marketed in the form of iron bars, lead, copper and tin ingots to the harbour of Les-Saintes-Maries-de-la-Mer (i.e. close to Arles antique city where large cargos were transferred to riverboats) and then shipped all the way to northern Gaul and the Germanic border (Delqué-Količ et al., 2017; Long and Domergue, 1995; Trincherini et al., 2001). Furthermore, in Arles, the water distribution system was operated by lead pipes (so-called *fistulae*) on each side of the Rhône, but also submerged across the Rhône stream to provide water to the prosperous Trinquetaille district (Long, 2009). In that regard, Delile et al. (2014) have shown that lead isotopes in sediments from the harbour of Imperial Rome enabled them to register the presence of the anthropogenic imprint induced by the presence of lead *fistulae* used in ancient Rome. Such lead contamination of the sediment by *fistulae* should also operate in Arles and thus be traced within the Rhône mud belt. Even though possible lead contamination by cities, such as Lyon or Narbonne should not be excluded, since they played a major role in merchant shipping during the Roman Period. To date no information is available regarding their water distribution system being operated by lead pipes.

Origin of the lead recorded in the sediments of the Gulf of Lions over the Holocene

In order to assess the origin of lead contaminations over the Holocene and get insight into the contamination processes, the $^{204}Pb/^{206}Pb$ and $^{207}Pb/^{206}Pb$ have been compared to several distant ore deposits (Figure 5(a)). Lead isotope compositions vary from one ore deposit to another, thus sediments, metal ores and most metal artefacts that contain traces of Pb (copper, tin, silver, gold, iron) can be fingerprinted. One should note that similar geology among different source regions might produce overlapping isotope characteristics (see Villa (2009) and Bode et al. (2009) for reviews). Furthermore, no significant fractionation of Pb isotopes results from the smelting and refining of Pb ore concentrates (Baron et al., 2009). The binary diagram (Figure 5(a)) clearly shows that the local ore deposits from the Cévennes more precisely from the Mont Lozère (Baron et al., 2006), match some post-Roman sediment sample isotopic lead compositions. All post-Roman sediment sample isotopic signatures lie in-between two end-members: a pre-Roman Holocene background and the Cévennes ores (Figure 5(a)). One should note that, natural sedimentation within the mud belt induces a mixing of lead particles from a natural Holocene background and potentially several

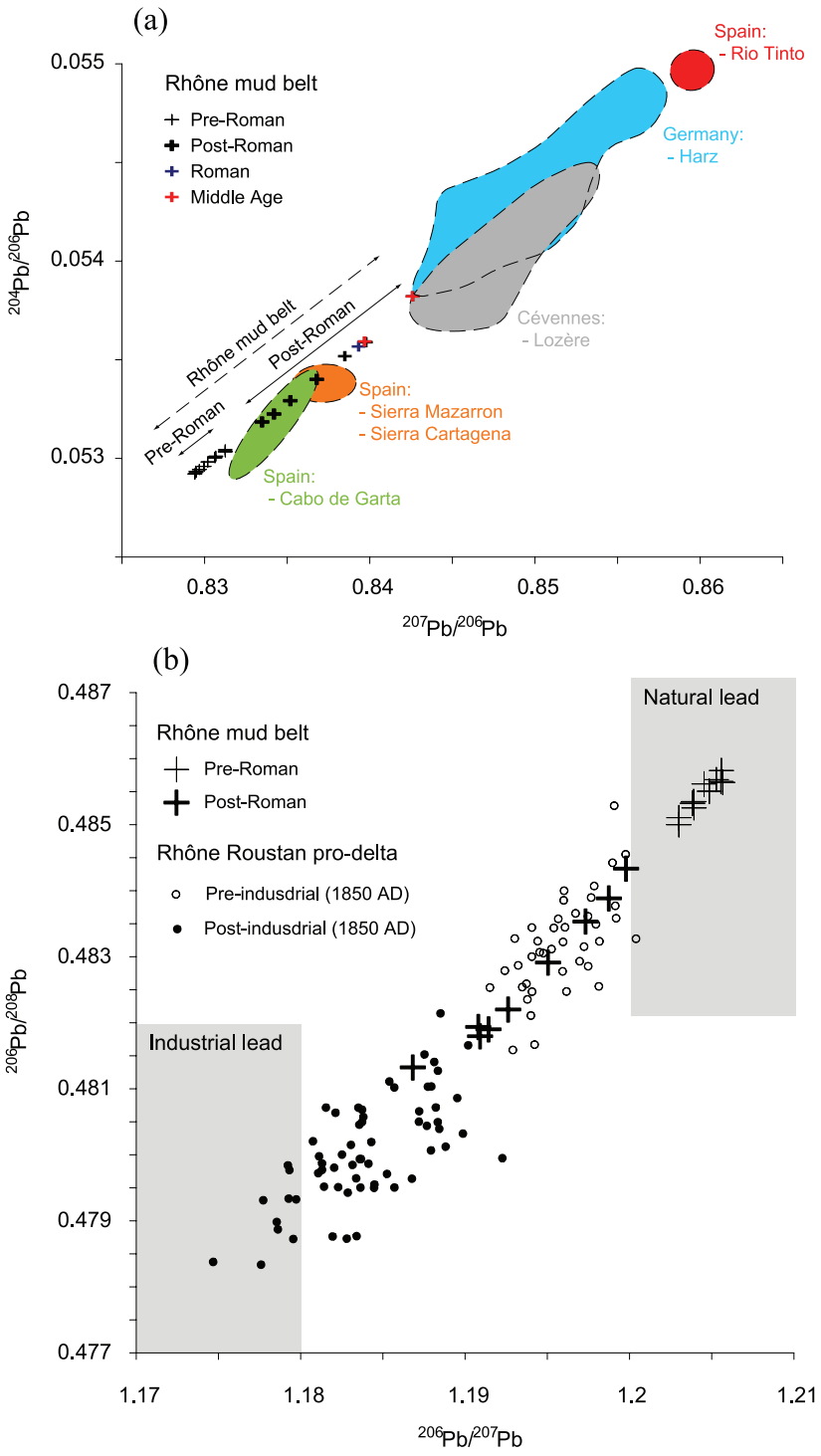


Figure 5. (a) Binary diagram showing sediment samples from Core KSGC-31 and ore deposits (coloured ellipses) from the Cévennes (Mont Lozère: Baron et al., 2006), ore deposits from Spain (Cabo de Garta and Sierra Mazzaron: Stos-Gale et al., 1995; Cartagena: Graeser and Friedrich, 1970; Rio Tinto: Marcoux, 1998; Pomiès et al., 1998; Stos-Gale et al., 1995) and ore deposits from Germany (Harz; Brockner, 1989; Lévêque and Haack, 1993; Tischendorf et al., 1992; Wedepohl et al., 1978; Zwicker et al., 1991). (b) Binary diagram showing lead isotopic data from the Rhône pro-delta sediments over the last 400 years (Cossa et al., 2018) compared to pre- and post-Roman Core KSGC-31 samples.

anthropogenic sources. Unlike other known regional mining sites such as the Montagne Noire known for iron (Baron et al., 2011; Domergue et al., 1993) and the Corbières known for iron but also for silver (Pb-Ag) and copper (Mantenant, 2014), the Mont Lozère is, to our knowledge, the only site that displays evidences of important silver-lead mining and smelting dating from the Gallic and Roman periods (Baron et al., 2005). To investigate further the well-accepted hypothesis according to which mine exploitation-derived aerosol lead particles from Spain spread across Europe, we compared KSGC-31 isotopic data with those distant Spanish ore deposits (Cabo de Garta and Sierra Mazzaron: Stos-Gale et al., 1995; Sierra Cartagena: Graeser and Friedrich (1970); Rio Tinto: Marcoux, 1998; Pomiès et al., 1998; Stos-Gale et al., 1995). Even though a mixture of lead from different Spanish sources cannot be excluded, since KSGC-31 post-Roman isotopic lead samples match some Spanish ore deposits (Rosman et al., 1997 and references therein), the local origin, that is, the Cévennes, is more likely in this case. To achieve completeness. The origin of Roman lead ingots from several wrecks immersed off-shore Les Saintes-Maries-de-la-Mer have been proven to be

of German origin (see Baron et al., 2011 for a review), thus strengthening the hypothesis of commercial trade between the Northern Occidental part of the Mediterranean Basin and western Europe (Delqué-Količ et al., 2017). These recent archaeological results are coherent with lead isotopic signatures of post-Roman sediment samples from Core KSGC-31 lying in between a German ore cloud (Brockner, 1989; Lévêque and Haack, 1993; Tischendorf et al., 1992; Wedepohl et al., 1978; Zwicker et al., 1991) and a pre-Roman background (Figure 5(a)). To conclude, a mix of several sources of contaminations are suggested: (1) the release of lead particles during extraction and smelting occurring around the Cévennes region, (2) Roman lead ingots of German origin immersed in front of the Rhône River mouths, (3) *fistulae* made of lead potentially originating from the Cévennes and Germanic ores crossing the Rhône River in Arles.

The Core KSGC-31 $^{206}Pb/^{207}Pb$ record shows an abrupt drop towards 1.192 around the beginning of the High Middle Ages period that also accounts for a clear source change (Figure 4(b)) as well as an increase in lead concentration (Figure 4(a)). Such a drop in $^{206}Pb/^{207}Pb$ has also been recorded in Sweden (Brännvall et al., 1997; Renberg et al., 1994; Figure 4(e)) and Greenland (Hong et al., 1994; Rosman et al., 1997; Figure 4(c) and (d)). This source shift and increase in lead concentration is concomitant with silver production in Germany (Settle and Patterson, 1980; Figure 4(f)); however, it should be noted that silver and lead are frequently co-occurring in ores. Historically, mining of the Rammelsberg ore (Harz Mountains; Germany) was fully established by 982 cal. a BP and continued until ~700 cal. a BP (Mohr, 1978; Monna et al., 2000). The binary diagram (Figure 5(a)) shows that a distant source originating from German ore deposits cannot be fully excluded since the very scattered German ore cloud matches one KSGC-31 Medieval isotopic samples (Brockner, 1989; Lévêque and Haack, 1993; Tischendorf et al., 1992; Wedepohl et al., 1978; Zwicker et al., 1991). However, the Mont Lozère Massif is considered to be the largest Medieval site of Pb-Ag metallurgical activities for extraction and smelting in France (Baron et al., 2006; 930−995 cal. a BP) and its associated lead isotopic signature matches Core KSGC-31 samples from the same period closely (Figure 5(a)). Regarding the potential contamination vector, the Mont Lozère is drained by a minor tributary of the Rhône (via the Ardèche River; Figure 1(a)) called Altier that ultimately flows into the Mediterranean. On a larger frame from the middle of the 11th to the middle of the 14th centuries AD in Europe, there was a need for Lead, Copper, as well as Silver for coinage purposes (Bailly-Maître et al., 2013). Consequently, several mining sites developed in central and southern France (Bailly-Maître et al., 2013), particularly across the Cévennes massif and the Montagne Noire, where ores display close lead isotopic signatures (Brévart et al., 1982; LeGuen and Lancelot, 1989; Marcoux and Brill, 1986). Those historical data are coherent with the sediment lead contamination recorded in the Gulf of Lions.

Marine sediments give access to continuous anthropogenic archives. In that regard, lead isotopic data from the Rhône prodelta sediments over the last 400 years (Cossa et al., 2018) has been compared to pre- and post-Roman core KSGC-31 data (Figure 5(b)). Core KSGC-31 post-Roman lead isotopic ratios lie in-between two end-members that are (1) sediments deposited before 2000 cal. a BP (>1.20) that represent the natural Holocene background and (2) sediments deposited after AD 1850 that are contaminated by European gasoline and industrial Pb pools (<1.18).

Conclusion

Core KSGC-31 was retrieved in the mud belt of the Gulf of Lions and provides a continuous sedimentary record over the Holocene period. The effect of natural climatic changes, as well as possible human-induced erosion on the sedimentation have been investigated with the use of sedimentation rates, chemical weathering (stable vs labile phases; Al_2O_3/K_2O) and sediment-source shifts (neodymium isotopic ratios; εNd). Elemental and isotopic lead was measured to record and trace contamination over the Holocene.

A major change in sedimentation centred around 4000/3000 cal. a BP has been observed in several proxies, including (1) an increase in sedimentation rates, (2) Al_2O_3/K_2O variations due to variations in chemical weathering with a low steady state until 4200 cal. a BP indicating low weathering conditions, as opposed to overall higher and fluctuating values from 4200 cal. a BP onwards indicating higher chemical weathering, (3) changes in εNd attributed to shifts in sediment supply where high εNd values are recorded in Core KSGC-31 and imply relatively higher sedimentary input from the Alpine crystalline massifs compared to the dominant Rhône and Languedoc background sedimentation, then from ~3000 cal. a BP onwards, a change is observed from a stable sediment source supply towards more fluctuating source-shift supply. Those fluctuations are consistent with climate changes occurring at that period. Besides, a possible human impact on soil disruption reinforcing sedimentation changes in the Gulf of Lions can be suggested.

$^{206}Pb/^{207}Pb$ drops around 2000 and 1000 cal. a BP suggest a clear change in lead source during the beginning of the Roman Empire and the beginning of the High Middle Ages. This record matches outstandingly well the atmospheric lead contamination recorded in Swedish lake sediments and Greenlandic ice cores, as well as periods of historical lead production. The well-accepted hypothesis that exploitation-derived aerosol lead particles from Spain during the Roman period and from Germany during the Medieval Period spread across Europe has been put to the test. Even though an input of lead from Spanish and German distant sources cannot be excluded according to their isotopic signature, the local origin is more likely in this case, that is, the Cévennes massif, and matches historical mining records in the area. The thirty-year academic debate concerning the origin of the lead ingots of the Saintes-Maries-de-la-Mer (Baron et al., 2011; Long and Domergue, 1995; Rothenhöfer, 2003; Trincherini et al., 2001) have shown that the quantitative fingerprinting approaches do not entirely grasp the complexity of a scientific question and therefore, an archaeological background is essential to achieve completeness. Therefore, rather than pointing to a definite source, on a bigger picture, our lead data suggest an intensification of the merchant shipping in the Northern Occidental part of the Mediterranean Basin during the Roman Period.

Acknowledgements

We owe many thanks to the GMO2-CARNAC cruise leaders Michel Voisset and Nabil Sultan, the captain and the crew of the R/V Le Suroit and the Plateforme d'Analyse des Sédiments du Laboratoire Géodynamique et Enregistrements Sédimentaires. Mickael Bode, from the Museum of Bochum, is thanked for providing access to its archeo-metallurgical database. Sandrine Baron and Gaspar Pagès, from the CNRS UMR5608 and UMR7041, are acknowledged for their valuable suggestions regarding the archeometallurgy. Enorma Omoregie, Bryan Killingsworth and Hannah Brightley are thanked for polishing the English on the different versions of the manuscript. We thank the three reviewers for their valuable comments.

Funding

The author(s) received no financial support for the research, authorship and/or publication of this article: This study is an outcome of a post-doc grant from IFREMER's Scientific Division and Institut Carnot Edrome.

ORCID iD

Jean Nizou https://orcid.org/0000-0003-3847-5637

References

Alfonso S, Grousset F, Massé L et al. (2001) A European lead isotope signal recorded from 6000 to 300 years BP in coastal marshes (SW France). *Atmospheric Environment* 35: 3595–3605.

Aloïsi JC, Auffret GA, Auffret JP et al. (1977) Essai de modélisation de la sédimentation actuelle sur les plateaux continentaux français. *Bulletin de la Société géologique de France S-XIX* 7: 183.

Arnaud F, Poulenard J, Giguet-Covex C et al. (2016) Erosion under climate and human pressures: An Alpine lake sediment perspective. *Quaternary Science Reviews* 152: 1–18.

Arnaud F, Révillon S, Debret M et al. (2012) Lake Bourget regional erosion patterns reconstruction reveals Holocene NW European Alps soil evolution and paleohydrology. *Quaternary Science Reviews* 51: 81–92.

Arnaud-Fassetta G (1998) *Dynamiques fluviales holocènes dans le delta du Rhône*. Thèse de 3ème cycle en géographie physique, Université de Provence (Aix-Marseille 1), Presses Universitaires du Septentrion.

Arnaud-Fassetta G (2002) Geomorphological records of a 'flood-dominated regime' in the Rhône Delta (France) between the 1st century BC and the AD 2nd century. What correlations with the catchment paleohydrology? *Geodinamica Acta* 15: 79–92.

Arnaud-Fassetta G, Carcaud N, Castanet C et al. (2010) Fluviatile palaeoenvironments in archaeological context: Geographical position, methodological approach and global change – Hydrological risk issues. *Quaternary International* 216: 93–117.

Bailly-Maître M-C, Minvielle Larousse N, Kammenthaler E et al. (2013) L'exploitation minière dans la vallée du Chassezac (Ardèche) : le plomb, l'argent et le cuivre au Moyen Âge (XIe-XIIIe siècles). *Archéologie Médiévale* 43: 11–40.

Bajard M, Sabatier P, David F et al. (2016) Erosion record in lake La Thuile sediments (preAlps, France): Evidence of mountain landscape dynamics throughout the Holocene. *The Holocene* 26: 350–364.

Baron S, Carigna J, Laurent S et al. (2006) Medieval lead making on Mont – Lozère Massif (Cévennes, France): Tracing ore sources using Pb isotopes. *Applied Geochemistry* 21: 241–252.

Baron S, Coustures M-P, Béziat D et al. (2011) Lingots de plomb et barres de fer des épaves romaines des Saintes-Maries-de-la-Mer (Bouches-du-Rhône, France): Questions de traçabilité comparée. *Revue Archéologique de Narbonnaise* 44: 71–98.

Baron S, Lavoie M, Ploquin A et al. (2005) Record of metal workshops in peat deposits: History and environmental impact on the Mont-Lozère Massif (France). *Environmental Science and Technology* 39: 5131–5140.

Baron S, Mahé-Le-Carlier C, Carignan J et al. (2009) Archaeological reconstruction of medieval lead production: Implications for ancient metal provenance studies and paleopollution tracing by Pb isotopes. *Applied Geochemistry* 24: 2093–2101.

Bassetti M-A, Berné S, Sicre M-A et al. (2016) Holocene hydrological changes in the Rhône River (NW Mediterranean) as recorded in the marine mud belt. *Climate of the Past* 12: 1539–1553.

Berné S, Jouet G, Bassetti MA et al. (2007) Late Glacial to Preboreal sea-level rise recorded by the Rhône deltaic system (NW Mediterranean). *Marine Geology* 245: 65–88.

Bode M, Hauptmann A and Mezger K (2009) Tracing Roman lead sources using lead isotope analyses in conjunction with archaeological and epigraphic evidence – A case study from Augustan/Tiberian Germania. *Archaeological and Anthropological Sciences* 1: 177.

Bond G, Kromer B, Beer J et al. (2001) Persistent solar influence on North Atlantic climate during the Holocene. *Science* 294: 2130–2136.

Brännvall M-L, Bindler R, Emteryd O et al. (1997) Stable isotope and concentration records of atmospheric lead pollution in peat and lake sediments in Sweden. *Water, Air, and Soil Pollution* 100: 243–252.

Brévart O, Duprés B and Allegre C (1982) Metallogenic provinces and the remobilisation process studied by lead isotopes: Lead– zinc ore deposits from the southern Massif Central, France. *Economic Geology* 77: 564–574.

Brisset E, Miramont C, Guiter F et al. (2013) Non-reversible geosystem destabilisation at 4200 cal. BP: Sedimentological, geochemical and botanical markers of soil erosion recorded in a Mediterranean alpine lake. *The Holocene* 23: 1863–1874.

Brockner W (1989) Archäometrische Untersuchungen an Fundmaterial aus Grabungen des Instituts für DenkmAlpflege Hannover. *Nachrichten aus Niedersachsens Urgeschichte* 58: 185–191.

Bruneton H, Arnaud-Fassetta G, Provansal M et al. (2001) Geomorphological evidences for fluvial change during the Roman period in the lower Rhône valley (southern France). *Catena* 45: 287–312.

Chapman MR and Shackleton NJ (2000) Evidence of 550-year and 1000-year cyclicities in North Atlantic circulation patterns during the Holocene. *The Holocene* 10: 287–291.

Cossa D, Cossa D, Fanget A-S et al. (2018) Chronology and sources of trace elements accumulation in the Rhône prodelta sediments (Northwestern Mediterranean) during the last 400 years. *Progress in Oceanography* 163: 161–171.

Cotten J, Le Dez A, Bau M et al. (1995) Origin of anomalous rare-earth element and yttrium enrichments in subaerially exposed basalts: Evidence form French Polynesia. *Chemical Geology* 119: 115–138.

Delile H, Blichert-Toft J, Goiran J-P et al. (2014) Lead in ancient Rome's city waters. *PNAS* 111: 6594–6599.

Delqué-Količ E, Leroy S, Pagès G et al. (2017) Iron Bar Trade between the Mediterranean and Gaul in the Roman Period: 14C Dating of Products from Shipwrecks Discovered off the Coast of Saintes-Maries-de-la-Mer (Bouches-du-Rhône, France). *Radiocarbon* 59: 531–544.

Deniel C and Pin C (2001) Single-stage method for the simultaneous isolation of lead and strontium from silicate samples for isotopic measurements. *Analytica Chimica Acta* 426: 95–103.

Domergue C, Cauuet B, Lavielle El, Pailler J-M et al. (1993) Un centre sidérurgique romain de la Montagne Noire. Le Domaine des Forges (Les Martys, Aude). In: Revue Archéologique Narbonnaise (ed.) *L'antiquité classique*. Paris: CNRS, p. 477.

Doyen E, Vanniere B, Berger J-F et al. (2013) Land-use changes and environmental dynamics in the upper Rhône valley since Neolithic times inferred from sediments in Lac Moras. *The Holocene* 23: 961–973.

Dufois F, Verney R, Le Hir P et al. (2014) Impact of winter storms on sediment erosion in the Rhone River prodelta and fate of sediment in the Gulf of Lions (North Western Mediterranean Sea). *Continental Shelf Research* 72: 57–72.

Elbaz-Poulichet F, Dezileau L, Freydier R et al. (2011) A 3500-year record of Hg and Pb contamination in a Mediterranean sedimentary archive (The Pierre Blanche Lagoon, France). *Environmental Science & Technology* 45: 8642–8647.

Fanget A-S, Berné S, Jouet G et al. (2014) Impact of relative sea level and rapid climate changes on the architecture and lithofacies of the Holocene Rhône subaqueous delta (Western Mediterranean Sea). *Sedimentary Geology* 305: 35–53.

Gauthier E, Richard H, Magny M et al. (2008) Le lac du Bourget (Savoie, France) à l'Age du Bronze: végétation, impacts

anthropiques et climat. Le peuplement de l'arc alpin. In: Richard H and Garcia D (eds) *Editions du CTHS (Documents préhistoriques)*, pp. 107–121.

Giguet-Covex C, Arnaud F, Poulenard J et al. (2011) Changes in erosion patterns during the Holocene in a currently treeless subAlpine catchment inferred from lake sediment geochemistry (Lake Anterne, 2063 m a.s.l., NW French Alps): The role of climate and human activities. *The Holocene* 21: 651–665.

Got H and Aloïsi J-C (1990) The Holocene sedimentation on the Gulf of Lions margin: A quantitative approach. *Continental Shelf Research* 10: 841–855.

Graeser S and Friedrich G (1970) Zur Frage der Altersstellung und Genese der Blei-Zink-Vorkommen der Sierra de Cartagena in Spanien. *Miner Depos* 5: 365–374.

Grossman EE, Eittreim SL, Field ME et al. (2006) Shallow stratigraphy and sedimentation history during high-frequency sea-level changes on the central California shelf. *Continental Shelf Research* 26: 1217–1239.

Hanebuth TJJ, Lantzsch H and Nizou J (2015) Mud depocenters on continental shelves – Appearance, initiation times, and growth dynamics. *Geo-Marine Letters* 35: 487–503.

Harnois L (1988) The CIW index: A new Chemical Index of Weathering. *Sedimentary Geology* 55: 319–322.

Hong SM, Candelone J-P, Patterson CC et al. (1994) Greenland ice evidence of hemispheric lead pollution 2 millennia ago by Greek and Roman civilizations. *Science* 265: 1841–1843.

Ivy-Ochs S, Kerschner H, Maisch M et al. (2009) Latest pleistocene and Holocene glacier variations in the European Alps. *Quaternary Science Reviews* 28: 2137–2149.

Jacob J, Disnar J-R and Bardoux G (2008) Carbon isotope evidence for sedimentary miliacin as a tracer of Panicum miliaceum (broomcorn millet) in the sediments of Lake le Bourget (French Alps). *Organic Geochemistry* 39: 1077–1080.

Jacobsen SB and Wasserburg GJ (1980) Sm-Nd isotopic evolution of chondrites. *Earth and Planetary Science Letters* 50: 139–155.

Jalali B, Sicre M-A, Bassetti M-A et al. (2016) Holocene climate variability in the North-Western Mediterranean Sea (Gulf of Lions). *Climate of the Past* 12: 91–101.

Jouet G (2007) *Enregistrements stratigraphiques des cycles climatiques et glacio-eustatiques du Quaternaire terminal. Modélisations de la marge continentale du Golfe du Lion*. PhD Thesis, Université de Bretagne Occidentale.

Lambeck K, Rouby H, Purcell A et al. (2014) Sea level and global ice volumes from the Last Glacial Maximum to the Holocene. *PNAS* 111: 15296–15303.

Lantzsch H, Hanebuth TJJ and Henrich R (2010) Sediment recycling and adjustment of deposition during deglacial drowning of a low accumulation shelf (NW Iberia). *Continental Shelf Research* 30: 1665–1679.

Le Roux G, Véron A and Morhange C (2005) Lead pollution in the ancient harbours of Marseilles. *Méditerranée* 104: 31–35.

LeGuen M and Lancelot JR (1989) Origine du Pb/Zn des minéralisations du Bathonien Sud-Cevenole. Apport de la géochimie isotopique comparée du plomb des galènes, de leur encaissant et du socle. *Chronique de la recherche minière* 495: 31–36.

Lévêque J and Haack U (1993) Pb isotopes of hydrothermal ores in the Harz (Monograph series on Mineral Deposits 30). *Gebruder Borntraeger* 30: 197–210.

L'Homer A, Bazile F, Thommeret J et al. (1981) Principales étapes de l'édification du delta du Rhône de 7000 B.P. à nos jours; variations du niveau marin. *Oceanis* 7: 389–408.

Long L (2009) César, le Rhône pour mémoire: Vingt ans de fouilles dans le fleuve à Arles. *Acte Sud* 1: 396.

Long L and Domergue C (1995) Le véritable plomb de L. Flauius Verucla' et autres lingots. L'épave des Saintes Maries-de-la-Mer. *MEFRA* 107: 801–867.

McConnell JR, Wilson AI, Stohl A et al. (2018) Lead pollution recorded in Greenland ice indicates European emissions tracked plagues, wars, and imperial expansion during antiquity. *PNAS* 115: 5726–5731.

Mantenant J (2014) *Montagnes métallifères de Gaule méditerranéenne Approche archéologique et historique de la production des métaux en Languedoc occidental du début du second âge du Fer à la fin de période romaine (IVème s. av. n. è. – Vème s. de n. è.)*. PhD Thesis, University of Toulouse.

Marcoux E (1998) Lead isotope systematics of the giant massive sulphide deposits in the Iberian Pyrite Belt. *Mineralium Deposita* 33: 45–58.

Marcoux E and Brill H (1986) Héritage et sources des métaux d'après la géochimie isotopique du plomb. *Mineralium Deposita* 21: 35–43.

Mayewski PA, Eelco E, Rohling J et al. (2004) Holocene climate variability. *Quaternary Research* 62: 243–255.

Mohr K (1978) *Geologie und Minerallagerstätten des Harzes*. Stuttgart: E. Schweizerbart'sche Verlagsbuchhandlung (Nägele U. Obermiller).

Monna F, Hamer K, Leveque J et al. (2000) Pb isotopes as a reliable marker of early mining and smelting in the Northern Harz province (Lower Saxony, Germany). *Journal of Geochemical Exploration* 68: 201–210.

Nesbitt HW and Young GM (1982) Early Proterozoic climates and plate motions inferred from major element chemistry of lutites. *Nature* 199: 715–717.

Nizou J, Hanebuth TJJ, Heslop D et al. (2010) The Senegal River mud belt: A high-resolution archive of paleoclimatic change and coastal evolution. *Marine Geology* 278: 150–164.

Parker A (1970) An index of weathering for silicate rocks. *Geological Magazine* 107: 501–504.

Pin C and Santos Zalduegui JF (1997) Sequential separation of light-rare-earth elements, thorium and uranium by miniaturized extraction chromatography: Application to isotopic analyses of silicate rocks. *Analytica Chimica Acta* 339: 79–89.

Pomiès C, Cocherie A, Guerrot C et al. (1998) Assessment of the precision and accuracy of lead-isotope ratios measured by TIMS for geochemical applications: Example of massive sulphide deposits (Rio Tinto, Spain). *Chemical Geology* 144: 137–149.

Reiche P (1943) Graphic representation of chemical weathering. *Journal of Sedimentary Petrology* 13: 58–68.

Renberg I, Bindler R and Brannval M-L (2001) Using the historical and atmospheric lead-deposition record as a chronological marker in sediment deposits in Europe. *The Holocene* 11: 511–516.

Renberg I, Wik-Persson M and Emteryd O (1994) Pre-industrial atmospheric lead contamination detected in Swedish lake sediments. *Nature* 368: 323–326.

Révillon S and Hureau-Mazaudier D (2009) Improvements in digestion protocols for trace element and isotope determinations in stream and lake sediment reference materials. *Geostandards and Geoanalytical Research* 33: 397–413.

Révillon S, Jouet G, Bayon G et al. (2011) The provenance of sediments in the Gulf of Lions, western Mediterranean Sea. *Geochemistry, Geophysics, Geosystems* 12: 1–20.

Richter TO, van der Gaast S, Koster B et al. (2006) The Avaatech XRF Core Scanner: Technical description and applications to NE Atlantic sediments. In: Rothwell G (ed.) *New Techniques in Sediment Core Analysis*. London: Geological Society of London (Special Publications 267), pp. 39–50.

Roaldset E (1972) Mineralogy and geochemistry of Quaternary clays in the Numedal area, southern Norway. *Norsk geologisk tidsskrift* 52: 335–369.

Rosman KJR, Chisholm W, Hong S et al. (1997) Lead from Carthaginian and Roman Spanish mines isotopically identified in

Greenland ice dated from 600 B.C. to 300 A.D. *Environmental Science & Technology* 31: 3413–3416.

Rothenhöfer P (2003) Geschäfte in Germanien. Zur Ausbeutung von Erzlagerstätten unter Augustus in Germanien im frühen Prinzipat. *Zeitschrift für Papyrologie und Epigraphik* 143: 277–286.

Settle D and Patterson CC (1980) Lead in Albacore: Guide to lead pollution in Americans. *Science* 207: 1167–1176.

Sicre M-A, Jalali B, Martrat B et al. (2016) Sea surface temperature variability in the North Western Mediterranean Sea (Gulf of Lion) during the Common Era. *Earth and Planetary Science Letters* 456: 124–133.

Simonneau A, Chapron E, Garçon M et al. (2014) Tracking Holocene glacial and high-altitude Alpine environments fluctuations from minerogenic and organic markers in proglacial lake sediments (Lake BlancHuez, Western French Alps). *Quaternary Science Reviews* 89: 27–43.

Simonneau A, Doyen E, Chapron E et al. (2013) Holocene land-use evolution and associated soil erosion in the French Prealps inferred from Lake Paladru sediments and archaeological evidences. *Journal of Archaeological Science* 40: 1636–1645.

Smith DE, Harrison S, Firth CR et al. (2011) The early Holocene sea level rise. *Quaternary Science Reviews* 30: 1846–1860.

Stos-Gale Z, Gale NH, Houghton J et al. (1995) Lead isotope data from the Isotrace Laboratory, Oxford: Archaeometry data base 1, ores from the western Mediterranean. *Archaeometry* 37: 414–415.

Stuiver M, Reimer PJ, Bard E et al. (1998) INTCAL98 Radiocarbon Age Calibration, 24000–0 cal BP. *Radiocarbon* 40: 1041–1083.

Sultan N and Voisset M (2002) GMO2 - CARNAC cruise. *RV Le Suroît*. Available at: http://dx.doi.org/10.17600/2020080.

Tischendorf G, Förster H-J, Bielicki K-H et al. (1992) On the origin of Hercynian magmatites and ore deposits in the Erzgebirge: Crustal signatures. *Zentralblatt für Geologie und Paläontologie, Teil II* 1: 131–146.

Trincherini PR, Barbero P, Quarati P et al. (2001) Where do the lead ingots of the Saintes-Maries-de-la-Mer wreck come from? Archaeology compared with Physics. *Archaeometry* 43: 393–406.

Ulses C, Estournel C, Durrieu de Madron X et al. (2008) Suspended sediment transport in the Gulf of Lions (NW Mediterranean): Impact of extreme storms and floods. *Continental Shelf Research* 28: 2048–2070.

Van der Leeuw SE (2005) Climate, hydrology, land use, and environ-mental degradation in the lower Rhone Valley during the Roman period. *Comptes Rendus Geosci* 337: 9–27.

Vella C (1999) *Perception et évaluation de la mobilité du littoral holocène sur la marge orientale du delta du Rhône*. PhD Thesis, Aix-Marseille University.

Vella C, Fleury T-J, Raccasi G et al. (2005) Evolution of the Rhône delta plain in the Holocene. *Marine Geology* 222–223: 235–265.

Villa IM (2009) Lead isotopic measurements in archeological objects. *Archaeological and Anthropological Sciences* 1: 149–153.

Vogel DE (1975) Precambrian weathering in acid metavolcanic rocks from the Superior Province. Villebon Township, southcentral Quebec. *Canadian Journal of Earth Sciences* 12: 2080–2085.

Vogt T (1927) Sulitjelmafeltets geologi og petrografi. *Norges Geologiske Undersokelse* 121: 1–560.

Wanner H, Beer J, Bütikofer J et al. (2008) Mid- to Late Holocene climate change: An overview. *Quaternary Science Reviews* 27: 1791–1828.

Wanner H, Mercolli L, Grosjean M et al. (2014) Holoceneclimate variability and change: A data-based review. *Journal of the Geological Society* 172: 254–263.

Wedepohl KH, Delevaux MH and Doe BR (1978) *Contributions to Mineralogy and Petrology*. Available at: https://doi.org/10.1007/BF00375513.

White WM, Albarede F and Telouk P (2000) High-precision analysis of Pb isotope ratios by multi-collector ICP-MS. *Chemical Geology* 167: 257–270.

Wirth S, Glur B, Gilli L et al. (2013) Holocene flood frequency across the Central Alps – Solar forcing and evidence for variations in North Atlantic atmospheric circulation. *Quaternary Science Reviews* 80: 112–128.

Zwicker U, Gale NH and Stos-Gale Z (1991) Metallographische, analytische und technologische Untersuchungen sowie Messungen der Bleiisotope an Otto-Adelheid-Pfennigen und Vergleichsmünzen meist aus dem 9.-11. Jahrhundert. In: Hatz G, Hatz V, Zwicker U, et al. (eds) *Otto-Adelheid-Pfennige. Commentationes de Nummis Saeculorum IX-XI* (Nova Series 7). Stockholm: Almqvist & Wiksell International, pp. 59–146.